ISSN: 2414-1895 DOI: 10.6919/ICJE.202504_11(4).0005

Finite Element Analysis-Based Study on the Anti-Slip Performance of Titanium Hemostatic Clips

Ru Chen

University of Shanghai for Science and Technology, Shanghai 200093, China

Abstract

This study employs finite element analysis (FEA) using ABAQUS to establish a hemostatic clip-blood vessel contact model, investigating the effect of different friction coefficients on the clamping stability and relative slip behavior of the clip. Simulation results indicate that within a small displacement range (0–0.6 mm), the interface between the clip and the vessel remains stable without significant slip. However, when the clip displacement exceeds 0.6 mm, relative slip increases significantly, with lower friction coefficients (0.38 and 0.4) making slippage more likely, while higher friction coefficients (0.5 and 0.53) effectively suppress slip and enhance clamping stability. Further analysis reveals that as the friction coefficient increases, the critical displacement rises from 0.69 mm to 1.0031 mm, and the critical force increases from 0.009297 N to 0.011857 N, indicating that a higher friction coefficient improves clamping force and reduces slip. This study provides theoretical guidance for optimizing the friction characteristics of hemostatic clips, contributing to their stability and reliability in clinical applications.

Keywords

Finite Element Analysis (FEA); Hemostatic Clip; Friction Coefficient; Clamping Stability.

1. Introduction

Titanium-based hemostatic clips are extensively utilized in minimally invasive surgeries to clamp blood vessels for hemostasis or to regulate specific blood flow conditions [1],[2],[3]. These clips offer significant advantages over traditional suturing techniques by reducing surgical duration and lowering the risk of postoperative complications [4],[5]. Nonetheless, the anti-slip properties of these clips are critical in determining their clamping stability and overall effectiveness in achieving hemostasis [6]. Inadequate clamping can result in clip slippage during surgery, potentially causing re-bleeding. On the other hand, excessive clamping force or improper application can impose undue stress on the vessel wall, leading to vascular damage or tissue necrosis [7]. Consequently, the frictional characteristics of hemostatic clips are vital for ensuring stable clamping. A low friction coefficient may compromise clamping efficiency, resulting in vessel displacement or detachment and increasing the likelihood of postoperative vascular complications. Investigating the clamping performance of these clips under varying friction conditions is therefore crucial for refining clip design and improving clinical safety.

In recent years, finite element analysis (FEA) has become a widely used computational tool in the biomechanical study of medical devices. By creating finite element models, researchers can analyze the mechanical behavior of surgical devices to assess their stability and impact on vascular tissues. For example, Gasser et al.[8] developed a three-dimensional finite element model that incorporates the nonlinear properties of arterial walls to study stress distribution, identifying that areas of high stress concentration may elevate the risk of vascular injury. He et al.[9] used finite element methods to examine arterial damage during pre-dilation and stent expansion. Their research employed a hyperelastic damage model to describe the stress-strain response of arterial walls and plaques,

ISSN: 2414-1895 DOI: 10.6919/ICJE.202504_11(4).0005

simulating how plaque softening affects the stent deployment process. Li et al. [10] utilized FEA to analyze the mechanical behavior of vascular stents with periodic structures during inflation expansion. Their study, conducted using ABAQUS/Explicit, applied periodic boundary conditions to enhance computational efficiency and explored the relationship between internal stent pressure and expansion diameter, providing valuable insights for stent design and long-term mechanical stability. Wang et al. [11]employed finite element simulations to study the impact of stent implantation on cerebral aneurysms and aortic dissections. They developed a simulation framework for stent deployment and analyzed the role of flow-diverting devices in treating aneurysms. Their findings indicated that maximum stress was concentrated at the contact points between the stent's exposed metal rings and the arterial wall, offering essential data for optimizing stent design and improving surgical strategies. Ge et al. [12] designed and analyzed a novel endoscopic successive hemostasis and closing device, validating its structural stability and hemostatic performance through finite element analysis. Using nickel-titanium alloy as the primary material, they assessed the stress distribution under different loading conditions, demonstrating that the device could provide stable clamping force while minimizing tissue damage. Zhang et al. [13]studied a hydrogel-based vascular stapler, evaluating its structural stability and vascular adaptability using FEA. Their research compared fitting-type and sleeve-type designs, analyzing blood flow distribution, shear stress, and burst pressure.

Although previous studies have explored the mechanical behavior of medical devices in-depth, research on the influence of surface friction coefficients on the clamping stability of hemostatic clips remains limited. Specifically, investigations into the stress distribution on vessel walls under varying friction conditions and the slip tendencies of hemostatic clips are insufficient. Therefore, this study employs ABAQUS finite element software to establish a contact model between titanium-based hemostatic clips and blood vessels. The Mooney-Rivlin hyperelastic model is used to simulate vascular tissue behavior [14]. By setting different friction coefficient conditions, we analyze the stress distribution, clamping stability, and slip tendencies of the hemostatic clip during vessel clamping. The aim is to identify an optimal range of friction coefficients, providing theoretical support for improving the anti-slip performance of hemostatic clips and offering data-driven insights for enhancing their clinical safety. This research advances the understanding of the interplay between hemostatic clips and vascular structures, delivering critical theoretical frameworks and experimental evidence to guide the development and optimization of next-generation clip designs.

2. Finite Element Modeling

2.1 Geometric Model

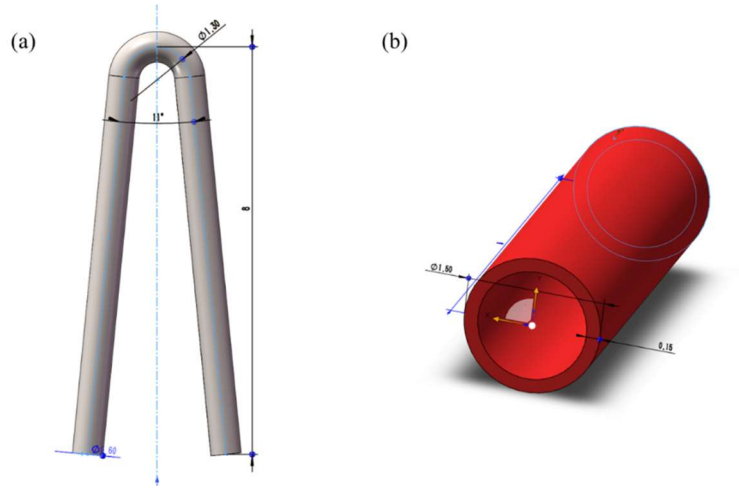

Figure 1. (a) Dimensions of the hemostatic clip model, (b) Dimensions of the blood vessel model

This research develops a finite element model to simulate the clamping interaction between a hemostatic clip and a blood vessel. The blood vessel is modeled as a cylindrical structure with an

ISSN: 2414-1895 DOI: 10.6919/ICJE.202504_11(4).0005

outer diameter of 1.5 mm and an inner diameter of 1 mm. The hemostatic clip is composed of pure titanium wire with a diameter of 0.6 mm, which is bent to form the clamping structure, as shown in Figure 1.

To compare the effect of the surface friction coefficient of the hemostatic clip on the mechanical behavior of the blood vessel, five sets of friction coefficients were selected for simulation analysis. The specific parameters are shown in Table 1.

Table 1. Assigned friction coefficients for the surface of the hemostatic clip model

Numble	μ
1	0.38
2	0.4
3	0.45
4	0.5
5	0.53

2.2 Page Numbers

The mechanical properties of the vascular wall are primarily influenced by the content and spatial configuration of elastic fibers, collagen fibers, and smooth muscle cells. Its nonlinear mechanical behavior is typically described using a hyperelastic material model. To analyze the biomechanical effects of the hemostatic clip on small arteries, the Mooney-Rivlin hyperelastic model was employed for finite element simulation, based on parameters from Reference [14]. The material parameters were set as follows: C_{10} = 18.90 kPa, C_{01} = 2.75 kPa, C_{20} = 85.72 kPa, and the incompressibility parameter d = 5×10^{-5}.The hemostatic clip is made of pure titanium, with an elastic modulus of 110 GPa and a Poisson's ratio of 0.34.

2.3 Interaction

In this finite element simulation, the contact between the hemostatic clip and the blood vessel is modeled as a surface-to-surface contact interaction, with the clip assigned as the master surface and the blood vessel as the slave surface, following a finite sliding formulation.The discretization method is set to surface-to-surface, with a smoothness parameter of 0.2. A dual contact constraint is applied to ensure accurate contact behavior.For tangential behavior, the Coulomb friction model is adopted, with a friction coefficient of 0.5, assuming isotropic friction to maintain uniform friction properties in all directions.For normal behavior, a linear pressure-overclosure model is used, with the default enforcement method and a contact stiffness value of 1200, ensuring stable interaction between the hemostatic clip and the blood vessel during clamping, as shown in Figure 2.

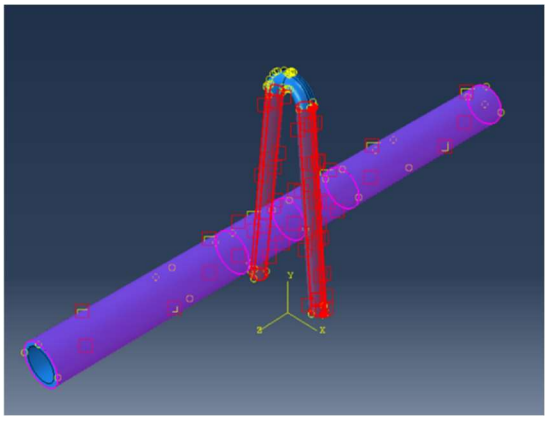

Figure 2. Surface-to-surface contact.

ISSN: 2414-1895 DOI: 10.6919/ICJE.202504_11(4).0005

The self-contact of the hemostatic clip is modeled using a self-contact method, with the contact surface set as the inner wall of the blood vessel. The surface-to-surface discretization method is selected, with a smoothness parameter of 0.2. A dual contact (path-based) constraint is applied to ensure numerical stability and accurately simulate the deformation characteristics of the hemostatic clip during clamping. For normal behavior, a linear pressure-overclosure model is adopted, with the enforcement method set to default and a contact stiffness value of 1200, as shown in Figure 3, ensuring sufficient contact stiffness during self-contact to prevent excessive deformation or numerical instability.

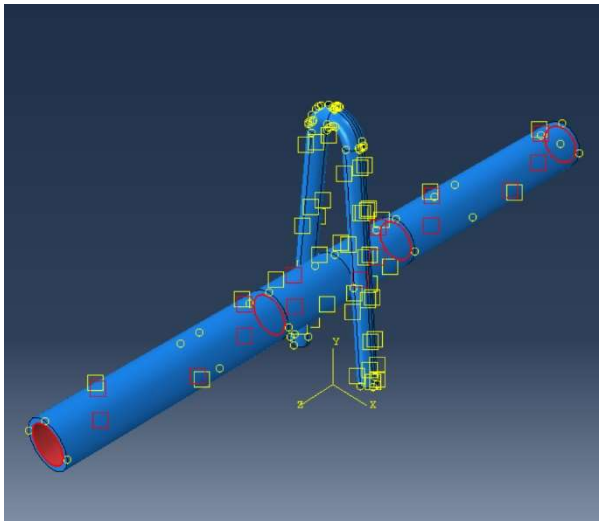

Figure 3. Blood vessel self-contact

The contact of the hemostatic clip is modeled using a standard contact method, with the contact surface set as the clip arms. The surface-to-surface discretization method is selected, with a smoothness parameter of 0.2. A dual contact constraint is applied to accurately simulate the real contact behavior of the blood vessel wall during the loading process. For normal behavior, a linear pressure-overclosure model is adopted, with the enforcement method set to default and a contact stiffness value of 115000, as shown in Figure 4, ensuring sufficient contact stiffness of the blood vessel wall under loading to prevent excessive deformation or numerical instability.

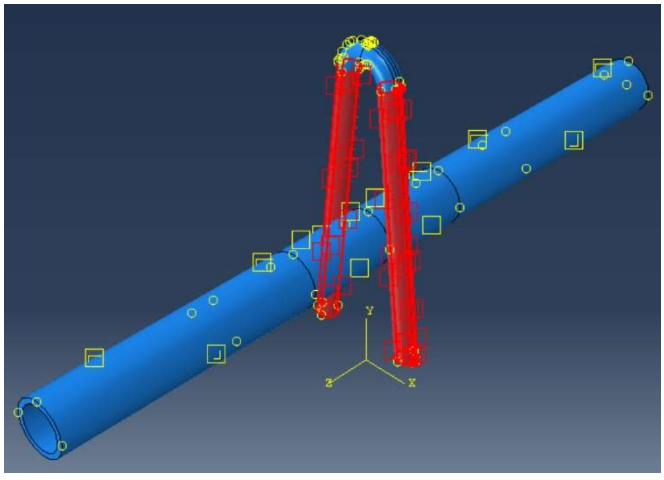

Figure 4. Hemostatic clip self-contact

ISSN: 2414-1895 DOI: 10.6919/ICJE.202504_11(4).0005

2.4 Boundary Conditions

To accurately simulate the clamping process of the hemostatic clip on small arterial vessels and analyze the mechanical response under different friction conditions, the following boundary conditions are set in the finite element analysis: a fixed constraint (Ux = Uy = Uz = 0) is applied at the distal end (outlet) of the vessel to prevent rigid body motion and ensure computational stability. The clamped section of the vessel is allowed to deform freely to replicate its actual deformation behavior during the clamping process. The hemostatic clip is loaded symmetrically, with both clip arms gradually contracting along the Y-axis to simulate the clamping process. A quasi-static analysis is performed with incremental displacement loading to ensure numerical stability. The nonlinear solution method is adopted, using the Newton-Raphson iterative algorithm to enhance computational accuracy. Automatic time step adjustment is enabled to ensure numerical convergence and computational efficiency.

3. Results

3.1 Static Mechanical Analysis

As shown in Figure 5(a), the Von Mises stress distribution of the blood vessel in its clamped state exhibits a maximum Mises stress of 0.37 MPa, concentrated on the lateral sides of the clamping contact region. This indicates that the highest mechanical load is exerted in this area, where the applied pressure from the hemostatic clip causes significant local deformation. The stress distribution is axisymmetric across the vessel cross-section, with lower stress levels observed in regions farther from the clamping site, suggesting that the mechanical influence of the hemostatic clip is primarily localized around the clamping points. Figure 5(b) provides a side view of the Mises stress distribution after vessel closure, offering a clearer visualization of the stress concentration at the clamping site. The stress is symmetrically distributed, with the highest stress localized at the clamping contact points. The vessel walls adjacent to the clip form distinct high-stress regions, where contact stress is significant, whereas the stress level in the center of the clamped section is slightly lower due to the contact surface shape influencing the stress distribution. As shown in Figure 5(c), the maximum principal stress distribution in the fully closed vessel indicates that the highest principal stress, approximately 0.15 MPa, occurs at the clamping region, suggesting that this area experiences considerable tensile stress. Figure 5(d) further reveals the internal stress distribution within the vessel wall, showing a distinct stress gradient between the inner and outer layers. The stress distribution across the vessel thickness is non-uniform, and localized shear stress accumulation may occur within the tissue during clamping, potentially affecting vascular mechanical stability. As illustrated in Figure 5(e), the variation of maximum principal stress with clamping displacement follows a nonlinear increasing trend. The X-axis represents the clamping displacement (mm), while the Y-axis represents the maximum principal stress (MPa). Within the 0–0.8 mm range, the increase in maximum principal stress is gradual, indicating that the vessel primarily undergoes elastic deformation, allowing it to buffer external forces. However, when the clamping displacement exceeds 1.0 mm, the maximum principal stress rises sharply, forming a steep curve, which signifies enhanced stress concentration. At the maximum clamping displacement of approximately 1.2 mm, the principal stress reaches its peak value of 0.40 MPa, indicating that the vessel wall has entered a high-stress state. This trend reflects the typical nonlinear mechanical behavior of biological tissues under external loads: within a certain range, the tissue can accommodate deformation through elasticity, but when the clamping displacement surpasses a critical threshold, stress escalates rapidly, potentially leading to irreversible damage or structural failure.Figure 5(f) presents the stress-strain curve for the vessel at the clamping site. The stress increases linearly in the 0.00–0.16 strain range, while beyond 0.16, the material enters a nonlinear region, ultimately reaching a maximum stress of 0.09 MPa.

ISSN: 2414-1895 DOI: 10.6919/ICJE.202504_11(4).0005

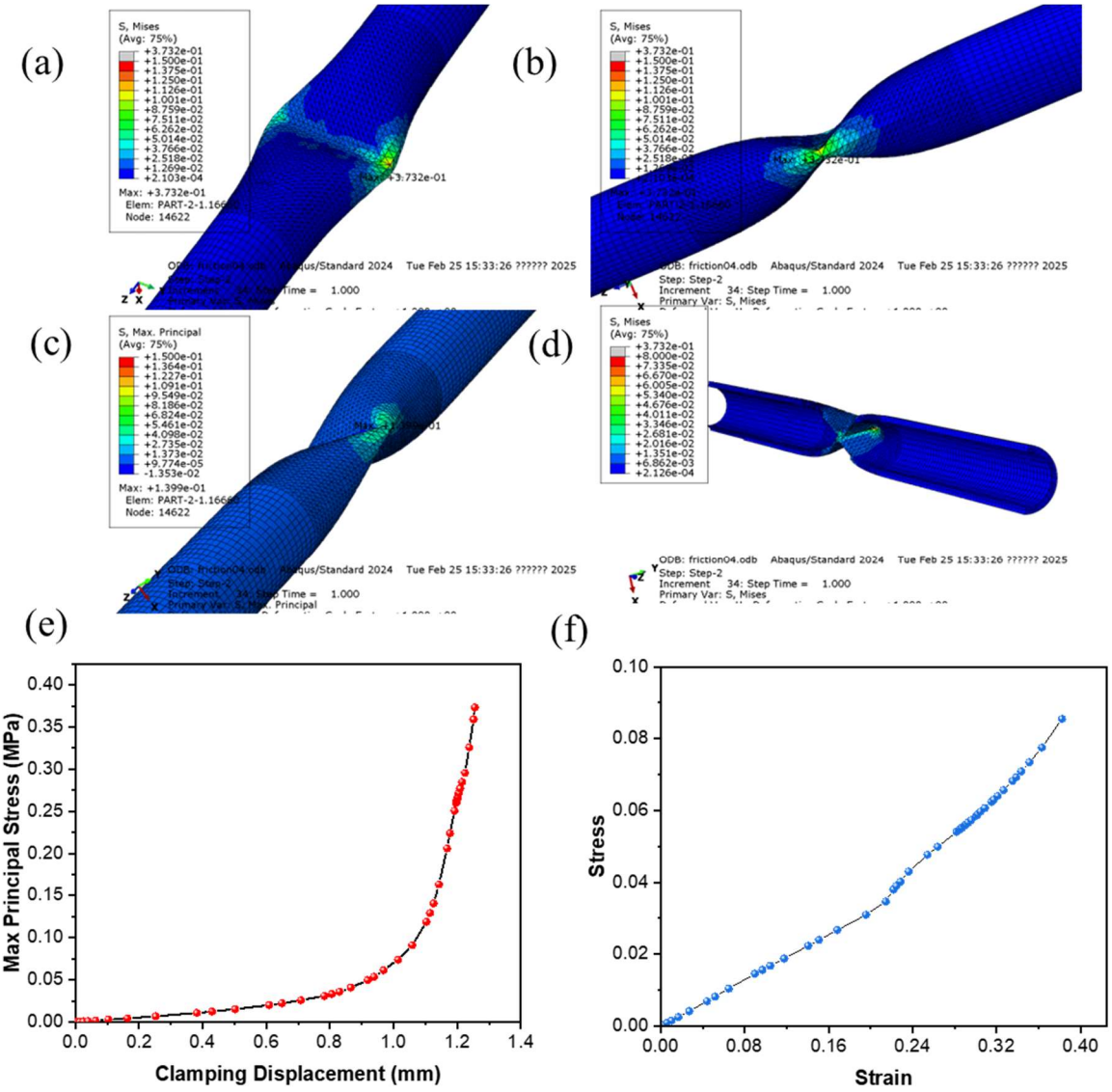

Figure 5. (a) Mises stress distribution after vessel closure, (b) Side view of Mises stress distribution after vessel closure, (c) Mises stress distribution in the fully closed and stabilized vessel, (d) Mises stress distribution in the vessel cross-section, (e) Maximum principal stress–clamping displacement curve, (f) Stress-strain curve

3.2 Dynamic Analysis

3.2.1 Slip Critical Force

As shown in Figure 6(a), when a small perturbation force is applied to the hemostatic clip clamping the blood vessel, Figure 6(b) illustrates the critical force for relative slip between the clip and the vessel under different friction coefficients. The critical displacement of the hemostatic clip increases gradually with the friction coefficient, measuring 0.69 mm, 0.7273 mm, 0.8485 mm, 0.9391 mm, and 1.0031 mm, corresponding to critical forces of 0.009297 N, 0.009362 N, 0.010141 N, 0.011052 N, and 0.011857 N, respectively. The overall trend indicates that a higher friction coefficient enhances clamping stability, requiring a larger displacement before the clip enters the slip state and corresponding to a higher critical force. This suggests that increasing friction effectively suppresses premature slippage of the clip, thereby improving its clamping reliability.

ISSN: 2414-1895 DOI: 10.6919/ICJE.202504_11(4).0005

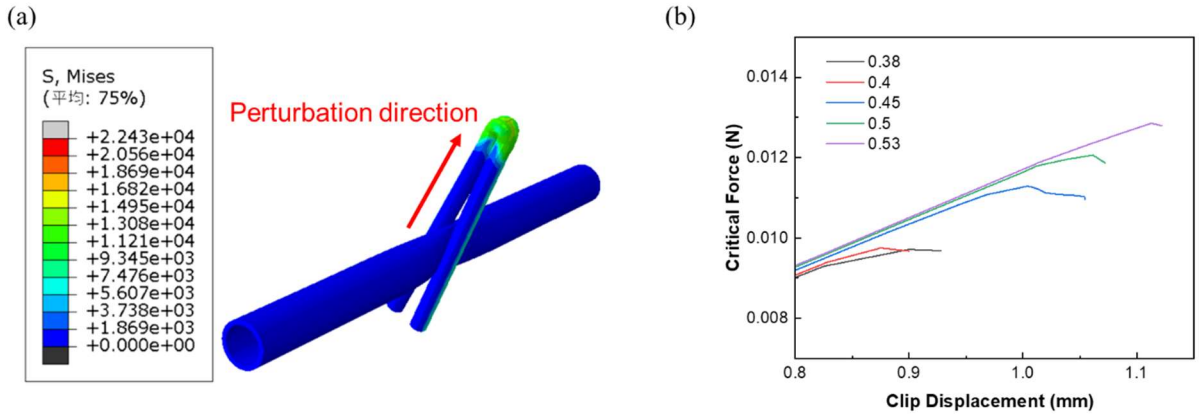

Figure 6. (a) Perturbation force applied to the hemostatic clip, (b) Critical force–displacement curve

3.2.2 Relative Slip

This section investigates the relationship between the traction force required for slight relative displacement between the hemostatic clip and the blood vessel and the friction coefficient. By simulating the minor slip of the clip relative to the vessel wall during clamping, the variation of frictional force under different friction coefficient conditions is analyzed to reveal the impact of friction characteristics on clamping stability. As shown in Figure 7, the relationship between clip displacement and relative displacement is presented, with different curves corresponding to various friction coefficients (0.38, 0.4, 0.45, 0.5, 0.53). Within the small displacement range (0–0.6 mm), the relative displacement remains close to zero, indicating a stable clamping interface with no significant slip. When the displacement of the clip reaches around 0.6 mm, the relative displacement begins to increase markedly, indicating that the clamping interface transitions into the slip phase, with lower friction coefficients promoting easier slippage. As the displacement further increases, the relative displacement follows a nonlinear growth pattern, where curves associated with lower friction coefficients (0.38 and 0.4) display a more pronounced rise, whereas higher friction coefficients (0.5 and 0.53) effectively mitigate slippage. These findings underscore the importance of friction properties in ensuring clamping stability, revealing that a higher friction coefficient contributes to minimizing relative slip and enhancing clamping reliability.

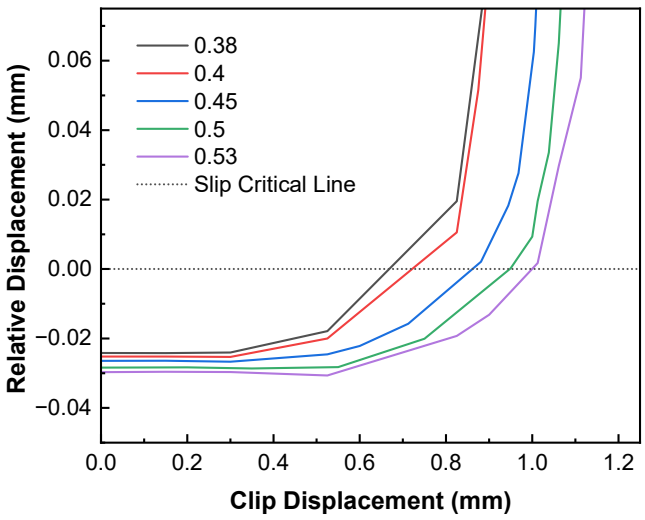

Figure 7. Critical Force for Hemostatic Clip Slippage

ISSN: 2414-1895 DOI: 10.6919/ICJE.202504_11(4).0005

4. Conclusion

This research employs finite element analysis (FEA) via ABAQUS to develop a contact model between a hemostatic clip and a blood vessel, aiming to explore how varying friction coefficients impact the clip's clamping stability and slip behavior. Simulations were conducted to analyze critical displacement, critical force, and slip patterns under different friction conditions, uncovering the role of friction coefficients in clamping performance. The findings indicate that within a limited displacement range (0–0.6 mm), the interaction between the hemostatic clip and the vessel remains stable, with no notable slippage observed. When the clip displacement exceeds 0.6 mm, relative slip increases significantly, with lower friction coefficients ($\mu = 0.38$ and 0.4) making slippage more likely, while higher friction coefficients ($\mu = 0.5$ and 0.53) effectively suppress slip and enhance clamping stability. Further analysis indicates that as the friction coefficient increases, the critical displacement increases from 0.69 mm to 1.0031 mm, and the critical force increases from 0.009297 N to 0.011857 N, demonstrating that a higher friction coefficient enhances clamping force and reduces slip. However, this also leads to localized stress concentration, affecting the biomechanical response of the blood vessel. This study quantifies the impact of the friction coefficient on the clamping stability of hemostatic clips, providing a theoretical basis for optimizing the frictional properties of these devices. The findings can serve as a reference for surface modification of hemostatic clips to improve their anti-slip performance and clinical reliability. This research is primarily based on finite element simulations and does not account for the complex mechanical behavior of vascular biological tissues or the influence of actual physiological conditions on clamping mechanics. Future work can incorporate experimental studies to further explore the effects of different surface treatments on friction performance, optimize the clamping effectiveness of hemostatic clips, and validate the reliability of numerical simulations.

4.1 Process

If you follow the “checklist” your paper will conform to the requirements of the publisher and facilitate a problem-free publication process.

Acknowledgments

Natural Science Foundation.

References

[1] Y. İ. Manavbaşı, H. Kerem, A. Erdem. The use of titanium clips in septal surgery for correction and strengthening, Journal of Plastic, Reconstructive & Aesthetic Surgery, vol. 65 (2012), 739-746.

[2] Z. Xi, Y.F. Wu, S.Y. Xiang, et al. Corrosion resistance and biocompatibility assessment of a biodegradable hydrothermal-coated Mg–Zn–Ca alloy: An in vitro and in vivo study, ACS Omega, vol. 5 (2020), 4548-4557.

[3] G. H. Lu, K. A. Selli. Temporary occlusion of the uterine artery at the origin using titanium clips for laparoscopic myomectomy, Journal of Minimally Invasive Gynecology, vol. 29 (2022), S65.

[4] M. Kuduvalli, K. E. McLaughlin, D. B. Trivedi, et al. Norwood-type operation with adjustable systemic–pulmonary shunt using hemostatic clip, The Annals of Thoracic Surgery, vol. 81 (2006), 1037-1039.

[5] A. Takeuchi, A. Uemura, S. Goya, et al. The utility of patent ductus arteriosus closure with hemostatic clip in dogs, Polish Journal of Veterinary Sciences, vol. 23 (2020), 255-260.

[6] Z. Saki, P. Kallidonis, Y. Noureldin, et al. Experimental studies of nonabsorbable polymeric surgical clips for use in urologic laparoscopy, Journal of Endourology, vol. 33 (2019), 730-735.

[7] B.P. Ooi, M.R. Hassan, K.K. Kiew, et al. Case report of a hemostatic clip being retained for 2 years after deployment, Gastrointestinal Endoscopy, vol. 72 (2010), 1315-1316.

[8] T.C. Gasser, R.W. Ogden, G.A. Holzapfel. Hyperelastic modelling of arterial layers with distributed collagen fibre orientations, J R Soc Interface, vol. 3 (2006), 15-35.

ISSN: 2414-1895 DOI: 10.6919/ICJE.202504_11(4).0005

[9] R. He, L.G. Zhao, V.V. Silberschmidt, et al. Finite element evaluation of artery damage in deployment of polymeric stent with pre- and post-dilation, Biomechanics and Modeling in Mechanobiology, vol. 19 (2020), 47-60.

[10] P.P. Li, R.J. Zhang. Finite element analysis of stent with periodic structure, Engineering Mechanics, vol. 29 (2012), 369-374.

[11] S.Z. Wang, Y.H. Cai, Z.Y. Meng, et al. Finite element simulation of stent implantation and its applications in the interventional planning for hemorrhagic cardio-cerebrovascular diseases, Sheng Wu Yi Xue Gong Cheng Xue Za Zhi, vol. 37 (2020), 974-982.

[12] S.C. Ge, C.L. Song, S.J. Yan, et al. Design and analysis of a novel endoscopic successive hemostasis and closing device, Journal of Medical Biomechanics, vol. 30 (2015), 416-420.

[13] H.J. Zhang, Y. Xiang, L. Mao, et al. Design and experimental study of vascular stapler based on hydrogel, Materials & Design, vol. 12 (2023), 357-365.

[14] K. John. Advances in Experimental Medicine and Biology (Springer International Publishing, 2018), p. 291.